Bulgarian Chemical Communications, Volume 52,Special Issue E (pp. 84 - 87) 2020

Mathematical modeling and experimental validation of advanced alkaline water electrolyser U/j performance

Galin Borisov, Nevelin Borisov, Elica Petkucheva, Evelina Slavcheva

Acad. Evgeni Budevsk Institute of Electrochemistry and Energy Systems - Bulgarian Academy of Sciences, Akad. G. Bonchev 10, 1113 Sofia, Bulgaria

Received April 07, 2020; Accepted April 27, 2020

Hydrogen generation by water electrolysis plays an important role in the green energy cycle with zero carbon emissions. The recent development in the classical alkaline electrolysis including the development of new electrode materials, novel cell architecture and system design, offers possibilities for enhanced kinetics and improved energy efficiency. At the same time, the mathematical modeling and simulations of the reaction mechanisms are more and more often used to predict the response of the system to varying operating conditions which in turn, speeds up additionally the progress of this clean energy converting technology. This paper presents a simple modeling of advanced alkaline water electrolyser using the theoretical thermodynamic functions and electrochemical equations by means of free Scilab 6.0 software. The model allows the calculation of the U/j characteristics as well as parameters such as reversible potential, activation and ohmic losses of the electrochemical process. It is validated using real experimental data obtained in a single electrolysis cell with Ni-based electrodes and Zifron Perl 500 diaphragm at 25 °C. Through extrapolation of the results obtained, the model is applied to predict the electrochemical performance of the cell at elevated temperatures up to 80 °C and current densities up to 1 A.cm^{-2}.

Keywords: Hydrogen production, alkaline electrolyser, U/j performance, mathematical modeling

INTRODUCTION

The renewable energy sources (wind, solar, etc.) are considered as zero emission technologies for electricity generation that will replace the carbon based economy. A major drawback of these technologies is their intermittent character. For this reason, the balancing of the electric grid is a real challenge as the unused electric energy needs to be curtailed. A promising solution for the problem is the usage of hydrogen generators as energy balancing consumers [1]. The advanced alkaline water electrolysers are considered as second-generation systems for industrial production of clean hydrogen. This type of electrical energy convertors have been successfully upgraded in the last years concerning energy efficiency, electron and mass transport balance, size, weight, etc. [2]. The principal scheme of the advanced alkaline water electrolyser is presented in fig. 1.

The hydrogen generators with alkaline electrolyte consist of two chambers separated by OH- conductive diaphragm also called separator. The system operates with metal mesh electrodes (stainless steel or nickel-based) with large surface area. The water splitting reaction (eq. 1) is an endothermic process and in order to proceed it requires energy.

$$H_2O + energy = H_2 + \frac{1}{2}O_2 \qquad (1)$$

The partial electrochemical reactions occurring on the anode and cathode of the cell are presented with equations (2) and (3), respectively.

Anode reaction:

$$2OH^-_{(aq)} \rightarrow \frac{1}{2}O_{2(g)} + H_2O_{(l)} + 2e^- \qquad (2)$$

Cathode reaction:

$$2H_2O_{(l)} + 2e^- \rightarrow H_{2(g)} + 2OH^-_{(aq)} \qquad (3)$$

Each partial reaction in turn, goes through number of consecutive steps described in the literature [3].

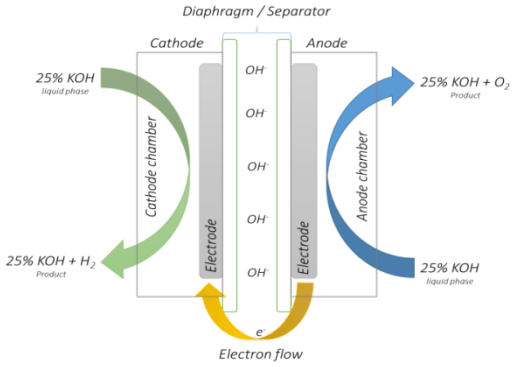

Fig.1. Principal scheme of advanced alkaline water electrolyser in a single cell mode

In order to split the water molecule to hydrogen and oxygen (according eqs. 2 and 3), an electric current flow (DC) is needed between both

* To whom all correspondence should be sent.
E-mail: gal.rusev@iees.bas.bg

electrodes. The hydrogen gas is produced on the cathode. Based on the fundamental thermodynamics and the basic electrochemical equations, the required minimum electric voltage to split the water electrochemically is determined by Gibbs equation (eq. 4):

$$\Delta G = zFErev \quad (4)$$

where ΔG is the Gibbs energy, $z -$ is the number of electrons and $F -$ Faraday constant, $Erev -$ reversible potential. $Erev$ is easily calculated by eq. (5):

$$Erev = \frac{\Delta G}{zF} \quad (5)$$

The reversible potential correlates with the generator temperature and reflects the thermodynamic effects of the electrochemical reaction. At standard conditions (25ºC, 1 atm) the value of $Erev$ is 1.229 V.

The water dissociation is also influenced by the catalytic activity of the electrodes. During the electrolysis process the cell voltage, $Ucell$, can be expressed as a sum of all potential barriers, namely the reversible potential, $Erev$, the activation potential of both partial reactions, $Eact,$ and the ohmic losses, $Eohmic,$ of the process. The mathematical relationship is presented by eq. (6).

$$Ucell = Erev + Eact + Eohmic \quad (6)$$

Both partial reactions according eqs. (2) and (3) have their own activation energy, while the activation energy of the electrochemical conversion is expressed by eq. (7).

$$Eact = slog(\frac{t1+\frac{t2}{T}+\frac{t3}{T^2}}{A} I + 1) \quad (7)$$

Theoretically, the activation overpotential, $Eact,$ increases with the increasing current density, while it can be decreased if active catalysts are integrated the both electrodes. In case of alkaline water electrolysis the transition metals such as Ni and its alloys have demonstrated high efficiency, resp. low overpotential, concerning both partial reactions [4-6].

The temperature dependence of the ohmic resistance (r) and the overvoltage (s) coefficients are described in details in the specialized literature [7]. The ohmic resistance of the advanced alkaline water electrolyser is related mainly to the low electrolyte conductivity. $Eohmic$ can be expressed as follows (eq. 8):

$$Eohmic = \frac{\delta}{ϙ} I \quad (8)$$

where δ is the thickness of the diaphragm (cm), ϙ is the cell conductivity ($S.cm^{-1}$) which strongly depends on the KOH concentration in the cell, and I is the operating current density.

This paper presents a simple modeling of advanced alkaline water electrolyser based on the partial electrode reactions in fig. 1, following the thermodynamic equations and dependencies expressed by eqs. (4-8). The mathematical calculations are performed using free Scilab 6.0 software. The energy requirements for the electrochemical conversion of water are calculated at KOH concentration and cell temperature input values fixed at 25 wt.% and 25 ºC, respectively. The results are validated using experimental data obtained in a patented single electrolysis cell [8] with highly advanced Ni based electrodes (both for anode and cathode) and possibility to operate at temperatures up to 120 ºC and pressure up to 5 bar.

EXPERIMENTAL

A. Mathematical modeling data

The mathematical modeling is performed using a free Scilab 6.0 software. The equations (4-8) are applied as programmable code directly in the Scinote (part of the software). The obtained dependencies are imported as data file in Origin 2019b in order to make precise comparison between the mathematical calculations and the real experimental data. The used variables are summarized in Table 1.

Table 1: Nomenclature of the used variables

Sym-bol	Parameters	Dimensions	Values
A	Area of electrode	[m^2]	0.0001
ΔG	Gibbs free energy	[$J.mol^{-1}$]	-
F	Faraday constant	[$C.mol^{-1}$]	96485
T	Temperature	[K]	293
V	Cell voltage	[V]	-
n	Number of cells	[n]	1
r	Ohmic resistance coefficient	[$\Omega.m^2$]	1
s	Coefficient for overvoltage on electrodes	[V]	0.185
z	Number of electrons	[n]	2
I	Current density	[$A.cm^{-2}$]	0 - 1
E_{rev}	Reversible potential	[V]	1.229

B. Advanced alkaline water electrolyser - preparation and assembling

In order to validate the developed mathematical model the performance of an advanced laboratory

alkaline electrolyser is evaluated experimentally in a single cell mode. The cell consists of two Ni-based electrodes with 7 cm^2 geometric area. They have a double layered structure - a gas diffusion support (Ni foam with 96% porosity) and 25 μm thick micro porous layer (mixture of Ni powder and PTFE at ration 70:30 wt.%; the preparation procedure is described in details elsewhere [9]). The diaphragm integrated in the cell is Zifron Perl (0.5 mm thick, 56% porosity). The electrolyte used is 25 wt.% KOH. The cell performance is characterized by *U/j* polarization curves recorded in range 0 $A.cm^{-2}$ to 0.1 $A.cm^{-2}$ (cell voltage) at scan rate of 1 $mA.s^{-1}$. The measurements are carried out using commercial Potentiostat/Galvanostat Gamry, model 1010E.

RESULTS AND DISCUSSION

The operation performance of the electrolyser is characterized by the change of the cell voltage as a function of the flowing current density, *j* ($A.cm^{-2}$). This dependence known also as voltammogram or *U/j* curve presents the response of electrolyser on varying electrical load. In this work the calculations and experiments are performed in the current density range from 0 $A.cm^{-2}$ to 1 $A.cm^{-2}$. The lower current density range requires low cell voltage and the system demonstrates high energy efficiency combined with low hydrogen production rate [10]. In fig. 2 are compared the model voltammogram calculated according eqs. (4-8) and the experimental curve obtained in the laboratory electrolysis cell at current density varying from 0 to 0.1 $A.cm^{-2}$.

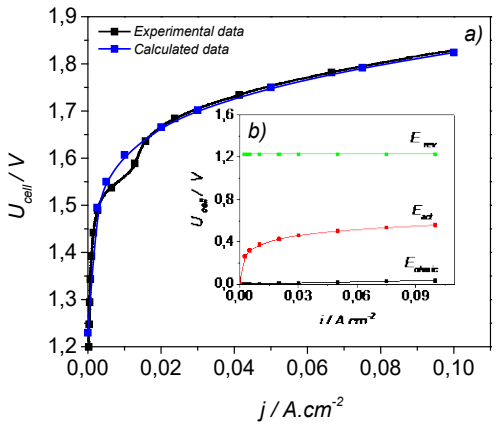

Fig. 2. Voltammograms of alkaline water electrolyser: a) comparison of mathematically calculated and experimental data; b) parameters, calculated by the developed model at 20 °C

Both voltammograms (experimental and modeled) fit perfectly, which validates the developed mathematical model. The increase of current density leads to increase in the cell overpotential. The process of hydrogen evolution starts at potentials of 1.6 V - 1.7 V where the current density value is 0.01 $A.cm^{-2}$ – 0.015 $A.cm^{-2}$. At these conditions, the cell overpotential calculated according eqs. (5) and (6) varies in the range 0.371 V to 0.471 V.

The parameters determining the cell voltage ($Erev$, $Eact$, $Eohmic$), are presented in fig.2b as function of the current density. It is seen that at low current densities the cell voltage strongly depends on the activation overpotential and the electrolysis starts at $Eact$ of about 0.35 V. The part of the cell voltage which is due to ohmic losses, $Eohmic$ is a linear function of current density and at low current densities it has much lower values compared to $Eact$.

In order to predict the behavior of the electrolyser at higher loads and elevated operating temperatures, the validated data from fig. 2 are applied in the model and the calculations are extended in the current density range up to 1 $A.cm^{-2}$ and temperatures up to 80 °C. The calculated results are presented in fig. 3.

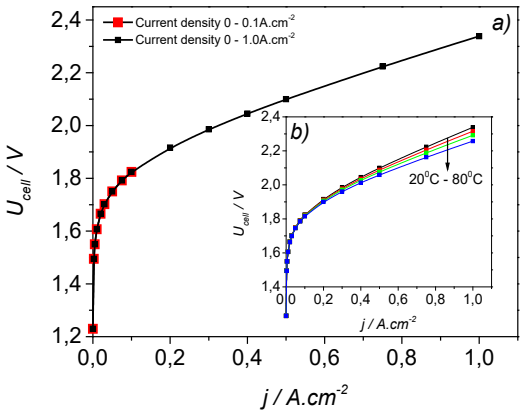

Fig. 3. U/j characteristics: a) experimental data (in red) and extended calculated U/j curve (in black) at current density up to 1 $A.cm^{-2}$; b) temperature dependence of the modeled U/j curves

It is seen that the increase of j leads to gradual change in the slope of the modeled U/j curve which above 0.2 $A.cm^{-2}$ becomes linear. At current density of 1 $A.cm^{-2}$ the cell voltage reaches value of 2.35 V.

The inset figure 3b shows the temperature dependence of the modeled U/j curves in the range 20 °C to 80 °C. The overall cell voltage depends essentially on the operating temperature. At current density of 1 $A.cm^{-2}$ it drops with approximate 10 mV per each 10 °C temperature increase.

The change of $Eohmic$ at these extended operating conditions (*j* up to 1 $A.cm^{-2}$ and temperature up to 80 °C) again demonstrates clear lineal dependency versus current density (fig. 4). At

current density of 1 A.cm^{-2} $Eohmic$ reaches values of 0.375 V at 20 ºC and is decreasing with approximately 20 mV per each temperature step of 20 ºC.

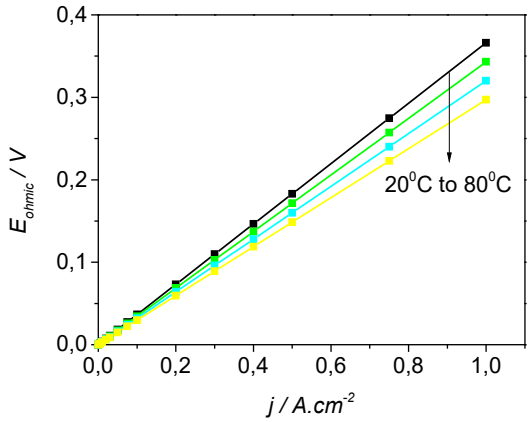

Fig. 4. Ohmic losses as function of current density at operating temperature range 20 ºC - 80 ºC

The respective calculations of $Eact$.as function of current density are shown in fig. 5. It is seen that the increase in cell temperature has impact on $Eact$, however it is much lower than on $Eohmic$ (fig. 5b).

It should be noted that the activation losses occur because the cell needs energy to initiate reactions at both electrodes - anode and cathode. As a result, a voltage drop is initialized inside the cell. With the increase of current density, the slope of the *U/j* curve changes. The activation polarization becomes less significant, while the ohmic effect becomes dominating.

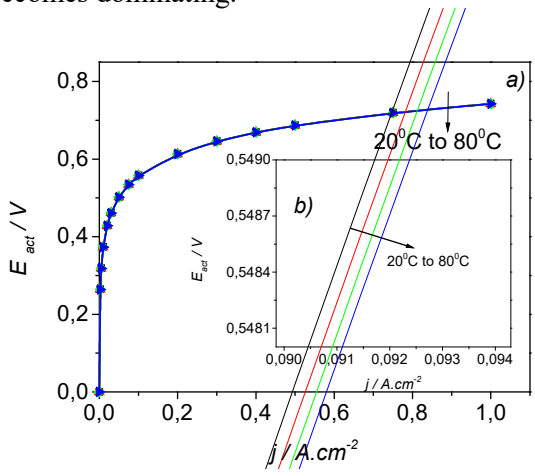

Fig. 5. Activation losses vs. current density: a) under operating temperature in range of 20 - 80 ºC, b) zoomed results in the potential range 548.0 mV – 549.0.V

CONCLUSIONS

The developed mathematical model based on fundamental thermodynamics and electrochemical relationships enables to calculate and predict electrochemical functions such as energy barriers, activation losses, ohmic drops and *U/j* performance characteristics of water electrolyser. It is validated through input of real experimental data obtained in advanced alkaline electrolysis cell and used to predict the cell performance at extended operating conditions namely, elevated cell temperatures and heavier electrical loads.

Acknowledgment: *This research is funded by the National Science Fund of Bulgaria, Contract КП-06-ОПР04. The experiments are performed using the equipment of distributed Research Infrastructure INFRAMAT (part of Bulgarian National Roadmap for Research Infrastructures) supported by Bulgarian of Education and Science under Contract DO1-155/28.08.2018*

REFERENCES

1. F. Martın, G. Hernandez, *Int. J. Hydrogen Energy,* **37,** 1151 (2012).
2. M. Schalenbach, O. Kasian, K. Mayrhofer, *Int. J. Hydrogen Energy,* **43,** 11932 (2018).
3. S. Marini, P. Salvi, P. Nelli, R. Pesentia, M. Villa, M. Berrettoni, G. Zangari, Y. Kiros, *Electrochim. Acta,* **82**, 384 (2012).
4. M. Kumar, N. Shetti, *Mater. Sci. Eng. Technol*., **1**, 160 (2018).
5. S. Ahn, H. Park, I. Choi, S. Yoo, S. Hwang, H. Kim, E. Cho, C. Yoon, H. Park, H. Son, J. Hernandez, S. Nam, T. Lim, S. Kim, J. Jang, *Int. J. Hydrogen Energy* **38**, 13493 (2013).
6. S. Hong, S. Ahn, J. Choi, J. Kim, H. Kim, H. Kim, J. Jang, H. Kim, S. Kima, *J. Appl. Surf. Sci,* **349**, 629 (2015).
7. Ø. Ulleberg, *Int. J. Hydrogen Energy,* **28**, 21 (2003).
8. G. Borisov, N. Borisov, E. Slavcheva, Bulg. Patent № 4341/ 2019
9. G. Borisov, A. Stoyanova, E. Lefterova, E. Slavcheva, *Bulg. Chem. Comm.,* **4**, 186 (2013).
10. S.Shiva Kumar, V. Himabindu, *Mater. Sci. Eng. Technol.,* **2**, 442 (2019).